Lipid Peroxides Promote Large Rafts: Effects of Excitation of Probes in Fluorescence Microscopy and Electrochemical Reactions during Vesicle Formation

Artem G. Ayuyan and Fredric S. Cohen

Rush University Medical Center, Department of Molecular Biophysics and Physiology, Chicago, Illinois

ABSTRACT   Raft formation and enlargement was investigated in liposomes and supported bilayers prepared from sphingomyelin (SM), cholesterol, and unsaturated phospholipids; NBD-DPPE and rhodamine-(DOPE) were employed as fluorescent probes. Rafts were created by lowering temperature. Maintaining 20 mol % SM, fluorescence microscopy showed that, in the absence of photooxidation, large rafts did not form in giant unilamellar vesicles (GUVs) containing 20 or more mol % cholesterol. But if photooxidation was allowed to proceed, large rafts were readily observed. In population, cuvette experiments, small rafts formed without photooxidation at high cholesterol concentrations. Thus, photooxidation was the cause of raft enlargement during microscopy experiments. Because photooxidation results in peroxidation at lipid double bonds, photosensitization experiments were performed to explicitly produce peroxides of SM and an unsaturated phospholipid. GUVs of high cholesterol content containing the breakdown products of SM-peroxide, but not phospholipid-peroxide, resulted in large rafts after lowering temperature. In addition, GUV production by electroswelling can result in peroxides that cause large raft formation. The use of titanium electrodes eliminates this problem. In conclusion, lipid peroxides and their breakdown products are the cause of large raft formation in GUVs containing biological levels of cholesterol. It is critical that experiments investigating rafts in bilayer membranes avoid the production of peroxides.

INTRODUCTION

The lipid components of biological plasma membranes are not uniformly distributed. They are thought to contain "rafts"—microdomains enriched in sphingolipids and cholesterol. Although positive identification of rafts in cell membranes has proven elusive, they are generally thought to exist and to concentrate proteins in regulated manners. When in rafts, proteins could quickly interact with each other to carry out their functions, and this is thought to occur in processes as diverse and far reaching as signal transduction and membrane trafficking (1–4). Most studies directed at characterizing rafts in cells have concluded that they are small, on the order of tens of nanometers (5–8). But a wide range of raft sizes has been reported (9,10) and rafts may constitute a large fraction of the area of a cell membrane (11).

Biological membrane rafts have been experimentally modeled using bilayer membranes that are rich in cholesterol and sphingomyelin (SM). Rafts definitely exist in these model lipid bilayer membranes (12,13). Fluorescent lipid probes that favorably partition into or that are excluded from bilayer raft domains are widely used to follow the formation and enlargement of rafts. Studies using video fluorescence microscopy have repeatedly shown that at temperatures below the solid-liquid transition temperature of the SM, the cholesterol and SM can phase separate into large microdomains (diameters in microns and larger) (14–16). Rafts, smaller than the resolution of an optical microscope, have also been detected in bilayer membranes by spectroscopy,

including fluorescence resonance energy transfer (FRET) (17–19) and NMR (20). Results of spectroscopy and microscopy have been combined to map phase diagrams for lipid compositions that phase separate into rafts (20,21). Combining these methods revealed a problem that has remained unresolved. It has been found that for some lipid compositions, spectroscopy reports that only small, nanometer-scale rafts should be present, whereas in fact large rafts are observed by video fluorescence microscopy.

This anomaly could have proven to be relatively inconsequential, but, in this study we show that the cause of the anomaly is actually of critical importance: excitation of fluorescent lipid probes leads to the generation of lipid peroxides that break down into products which dramatically alter raft properties. In particular, the generation of SM peroxide breakdown products can induce nanometer-scale rafts to grow to micron sizes. Our findings have wide-ranging consequences, since so much of the data used to describe the physics of rafts are based on fluorescence and microscopic methodologies. We also compare raft properties in giant unilamellar vesicles (GUVs) to those in planar lipid bilayers supported by a solid substrate. We find that photooxidation promotes raft enlargement in the same manner for GUVs and for bilayers separated from the substrate by a polymer cushion. But if the bilayer is directly adhered to the substrate, interactions between the lipid bilayer and substrate promote formation of large rafts. We conclude that when using fluorescence microscopy to study rafts, it is essential that photooxidation and all other causes of lipid peroxidation be stringently eliminated.

MATERIALS AND METHODS

Forming giant unilamellar vesicles

GUVs were prepared from egg SM (eSM), cholesterol, and dioleoylphosphatidylcholine along with fluorescent lipid probes, either Rho-DOPE or NBD-DPPE or both. All lipids were obtained from Avanti Polar Lipids (Alabaster, AL). GUVs were formed by electroswelling using standard techniques (22), modified to prevent lipid peroxidation. Briefly, a small amount of lipid dissolved in chloroform was deposited within a well (∼7-mm diameter) that was machined into a titanium plate (of thickness 2.5 mm). The chloroform was removed by a stream of argon followed by maintaining the plate under vacuum for 1 h. This plate and another titanium plate (without a well) were apposed, creating a capacitor; the plates were spaced apart by a 0.5-mM-thick Teflon sheet with a 15-mm-diameter hole and filled with an aqueous solution, usually 200 mM sucrose dissolved in 18 MΩ deionized water. For all procedures, solutions were purged of O_2, unless stated otherwise. GUVs were produced by electroswelling: a 10-Hz, 1.4-V p-p sine wave voltage was applied across the capacitor for 40 min at 55–60°C. This is above the 41°C transition temperature (T_m) of 16:0 SM, the major component of eSM. After forming GUVs, temperature was slowly lowered to 25°C and the suspension was collected.

Microscopic and fluorometric observation of rafts

A chamber with Peltier control of temperature was mounted on the fluorescence microscope stage. After adding a few microliters of the GUV sucrose solution to an isotonic glucose solution within the chamber, the GUVs rapidly settled onto the bottom coverslip of the chamber. The coverslip was pretreated with 10 mg/ml BSA for 5 min and then thoroughly rinsed (23) to prevent the GUVs from directly touching the glass and rupturing. A long-working-distance 63× oil immersion objective (numerical aperture 1.2, Zeiss, Thornwood, NY) was used to observe the GUVs. Images were captured with a cooled charge-coupled device camera (model DV 437 BV, Andor Technology, Belfast, United Kingdom) and stored to hard disk for later analysis. We operationally define domains enriched in NBD-DPPE and/or depleted in Rho-DOPE as rafts. To lower temperature below ∼25°C, we displaced the oil immersion objective from the coverslip. This thermally decoupled the chamber from the microscope and eliminated condensation onto the objective that would otherwise occur. After achieving the desired temperature, the objective was quickly adhered by oil to the coverslip for high resolution observation.

For fluorimetry (Luminescence Spectrometer LS50B, Perkin Elmer, Foster City, CA) within cuvettes, large unilamellar vesicles were prepared by extrusion (24) through filters (200-nm pores) inserted into a device designed for small volumes (LiposoFast, Avestin, Ottawa, Canada). Typically 1–2 mg of lipid in 0.5 ml of 10 mM Tris, pH 7.3, was extruded. For experiments, the solutions were purged of oxygen and the vesicle-containing cuvette was sealed from air. Temperature was controlled via a thermostated cuvette holder.

Supported bilayers

A lipid film of eSM/Chol/DOPC/DOPE (20:20:40:20%) was hydrated in 100 mM NaCl, 10 HEPES, pH 7.2, at 55–60°C for 1 h. After vortexing, the multilamellar lipid vesicles (MLVs) were sonicated for 10 min at 55–60°C within a cuphorn attachment to a cell disruptor that was set to continuous maximum power (Cell Disruptor 200, Branson, Danbury, CT) to create a suspension of small unilamellar vesicles (SUVs) that were added (∼0.5–1 mg lipid/ml) to a freshly cleaved mica slide. The SUVs contacting the mica surface ruptured and fused to spontaneously create, within 10 min, an adhered planar bilayer (25). We also prepared bilayers that were separated from the substrate by a polymer cushion. After depositing ∼40 μl of a 100 ppm polyethyleneimine (PEI) solution on the surface of the mica (∼50 mm²), the slide was washed with water and then dried at room temperature for several hours. A bilayer was made on the PEI-covered mica in exactly the same way as described, without polymer. A short chain PEI polymer (1800 D) and its cushioned bilayer have been characterized (26,27). We used this short PEI as well as a longer (65,000 D) version.

Production of lipid peroxides

Lipids can peroxidize at any double bond. Thus, illuminating fluorescent probes within a bilayer can peroxidize SM, cholesterol, and any unsaturated lipid. We produced peroxides of eSM and DOPC by preparing MLVs consisting solely of eSM or DOPC in 10 mM HEPES or in 10 mM Tris (pH 7.4). To generate peroxides, chlorophyllin—a semisynthetic derivative of chlorophyll—was added (at 10–20 μM) to an MLV suspension, and SUVs were created by sonication. (For eSM, all procedures were performed at 60°C.) Chlorophyllin is photoexcitable (i.e., it is a photosensitizer) and readily partitions into membranes (28); we produced lipid peroxides by illuminating the vesicles with a 5-mW red (650 nm) laser diode for 2 h.

The suspension of peroxidized vesicles was mixed with chloroform/methanol (2:1), and phase separation of these two solvents was accelerated by low-speed centrifugation. The lipid peroxides were enriched in the water/methanol phase, as determined by a ferrous oxidation in xylenol orange (FOX)-based assay. This phase was collected and both solvents were evaporated. The peroxide-containing material was dissolved in a methanol/water (9:1) solution. We catalyzed the full breakdown of the peroxides in a Haber-Weiss reaction by adding a small amount of 5 mM ammonium ferrous sulfate in 0.5 M sulfuric acid (final Fe^{2+} concentration ∼50–100 μM Fe^{2+}) (29). The products of this reaction are mostly hydroxylated compounds. To minimize any reaction cascades initiated by peroxide-produced free radicals, we included an excess (4 mM) of the antioxidant butylated hydroxyl toluene (BHT). BHT provides a substrate for hydrogen abstraction by lipid-free radicals, thereby minimizing any cross-linking between radicals. The breakdown products should thus consist almost exclusively of monomers. (Control experiments established that BHT did not produce rafts.) The reaction was allowed to proceed for 1 h. The acid was then neutralized with sodium carbonate, and an equal volume of chloroform was added. From the measured initial peroxide content, we found that at least half of the breakdown products were in the chloroform phase after the water and chloroform phase separated. We collected the products from this phase only to eliminate the considerable amount of ions (e.g., sodium, carbonate, and sulfate) that had been added as salts and acid. After evaporating the large volume of chloroform, we found that the breakdown products of SM-peroxide were not soluble in small volumes of any combination of chloroform, methanol, and water that we used. We suspended the products in chloroform/methanol (2:1) and solubilized them by adding water (∼0.25×), containing 50–100 μM Fe^{2+}, that had been acidified with either 10 mM sulfuric acid or 50 mM acetic acid. After the solubilization, we added $NaCO_3$ to neutralize the H_2SO_4; acetic acid is a weak acid and volatile, and thus, for this preparation, explicit reneutralization was not necessary. Phase separation of the solvents was accelerated by centrifugation. The products were now solubilized within the chloroform phase. We included these isolated breakdown products in a GUV-lipid mixture that does not otherwise generate large rafts (i.e., eSM/cholesterol/DOPC, 20:40:40%) to determine whether the product promoted large raft formation. Whenever including a product in a lipid mixture, we removed the same percentage of unoxidized component as product added (e.g., 15 mol % eSM was used if 5 mol % of SM-breakdown products were included) to simulate the oxidative processes during fluorescence microscopy. Phospholipid contents were quantified by a colorimetric assay (30). We used diethylenetriaminepentaacetic acid (DTPA) as a chelating agent to prevent autooxidations that could result from redox reactions between dioxygen and the trace iron that is invariably present; EDTA does not prevent these reactions, and in fact, it enhances them (29).

Lipid peroxide content assay

Peroxide content was quantified by slight modification of a FOX assay (31). The peroxide-containing material was dissolved in methanol and mixed with

100 μM xylenol orange, 250 μM ammonium ferrous sulfate, 5 mM
N-propyl gallate (NPG) or 4 mM BHT (as antioxidants), 25 mM sulfuric
acid in 90% methanol. The absorbance at 585 nm was used to calculate the
peroxide content. Measured amounts of n-butyl hydroperoxide were used to
generate a standard curve.

Peroxide production during electroswelling

We tested whether electrode reactions during preparation of GUVs resulted in
peroxide formation. We made these determinations for both titanium and the
traditional indium tin oxide (ITO)-glass as electrodes. GUVs were prepared by
electroswelling in a sucrose solution at 60°C. As a control, all steps of GUV
production were carried out, except voltage was not applied. Total phospho-
lipid content was used to normalize the lipid peroxide levels of each prep-
aration. To measure peroxide levels, a suspension of GUVs was diluted with
methanol and 75–150 μl of this sample was combined with an equal volume of
the FOX assay cocktail. The preparation was vortexed, sealed under argon, and
incubated at room temperature for 30 min in a FOX assay.

RESULTS

Photobleaching promotes formation of large rafts

We followed phase separation of lipids within bilayer
membranes by video fluorescence microscopy. Rho-DOPE
preferentially resides in domains rich in liquid-disordered
phases and is excluded from liquid-ordered domains (15);
NBD-DPPE preferentially partitions into liquid-ordered
domains (32). For bilayers containing SM and cholesterol,
we refer to domains enriched in NBD-DPPE and/or depleted
in Rho-DOPE as rafts. At temperatures above the T_m of eSM,
~41°C for 16:0 SM, fluorescence from Rho-DOPE or NBD-
DPPE was always uniform, indicating that large-scale phase
separation did not occur. As has been observed by many
(14,15,22,32), for some lipid compositions, microscopically
visible rafts form at temperatures below T_m, the precise
temperature required dependent on composition. We have
unexpectedly found that for some lipid compositions and
temperatures, microscopically observed phase separation is
caused by lipid oxidation during photoexcitation rather than
by intrinsic phase separation of pure, nonoxidized compo-
nents. For lipid compositions that intrinsically yield large
rafts, photooxidation augments the extent of raft enlarge-
ment and increases the line tension.

In Fig. 1, we illustrate the effects of photooxidation for
GUVs composed of 20% eSM, 40% cholesterol, and 40%
DOPC. (The percentage of DOPC was reduced to accom-
modate the amount of Rho-DOPE and/or the NBD-DPPE
included in the lipid mix.) The use of photoprotectors and
deoxygenated solutions is the standard method to minimize
photooxidation. In the presence of the photoprotector NPG,
optically detectable phase separation was not observed when
temperature was lowered to 25°C (Fig. 1 A) (rate of lowering =
3°C/min), nor when temperature was further lowered to
~10°C (Fig. 1 B). However, lowering temperature to ~1°C
induced phase separation for an appreciable fraction of the
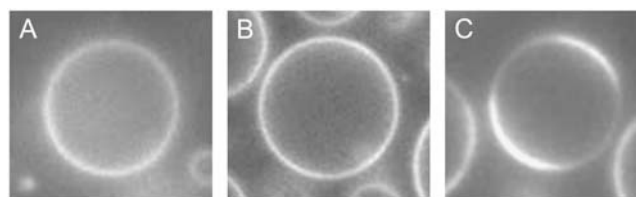GUVs (Fig. 1 C). These phenomena occurred independent of

FIGURE 1 Large rafts do not form for a high cholesterol-content
membrane in the absence of photooxidation, unless temperature is extremely
low. Rafts do not appear at 25°C (A) or 10°C (B), but some rafts do appear at
1°C (C). GUVs were formed from a 20:40:40% eSM/cholesterol/DOPC
mixture. NBD-DPPE was used as probe for each of these panels.

whether only one of the two probes was present, or both were
included in the lipid mix.

In contrast, large rafts appeared at 25°C within ~30 s of
illumination when photooxidation was not prevented (i.e.,
NPG was omitted) (Fig. 2). (We did not attempt to determine
the precise transition temperature for this photoinduced
process.) Large rafts for similar ratios of lipids have been
observed by several groups (14–16,33), although the precise
lipid mixture varies among laboratories. These photoinduced
rafts did not immediately form for all GUVs. Some GUVs
were spherical (i.e., circular in cross section) and these did
not exhibit a fluctuating membrane, indicating that the
vesicle was fully swollen and the membrane taut. Rafts
formed quickly upon illumination within these GUVs. Other
GUVs exhibited noncircular cross sections, and, for these,
their shape fluctuated, indicating an excess of membrane area
for the enclosed volume. For these latter GUVs, illumination
caused shape changes before raft formation. Patches of
membrane were observed to bud and some pinched off. In
the presence of antioxidants, none of these shape changes
occurred as a result of our intensity of illumination. Fluo-
rescence remained uniform during this period, indicating that
these patches were not rafts. The originally nonspherical
GUVs assumed a spherical shape that did not fluctuate once
the budded patches pinched off. Once GUVs were spherical,
large rafts were observed. We conclude that photoinduced
raft formation required that the GUV be spherical. All rafts
were fluid, mobile, and merged when they contacted each
other. Merger was the dominant means for creating large
rafts. The same photoinduced phenomena were observed for
photoprotected GUVs when light intensity was sufficiently
increased. In short, once membrane tension is nonzero,
photooxidation of lipid probes promotes the creation of large
rafts. Like the behavior of flaccid vesicles, the photoinduced
rafts often formed buds at the surface of the GUV and
sometimes pinched off. (At this point, only the rafts formed
buds.) This budding clearly shows that these rafts have large
line tensions, on the order of several piconewtons (33).

We tested the dependence of large raft formation on the
SM/cholesterol percentages in GUVs when photooxidation
was prevented. For SM/cholesterol percentages of 20:10%,
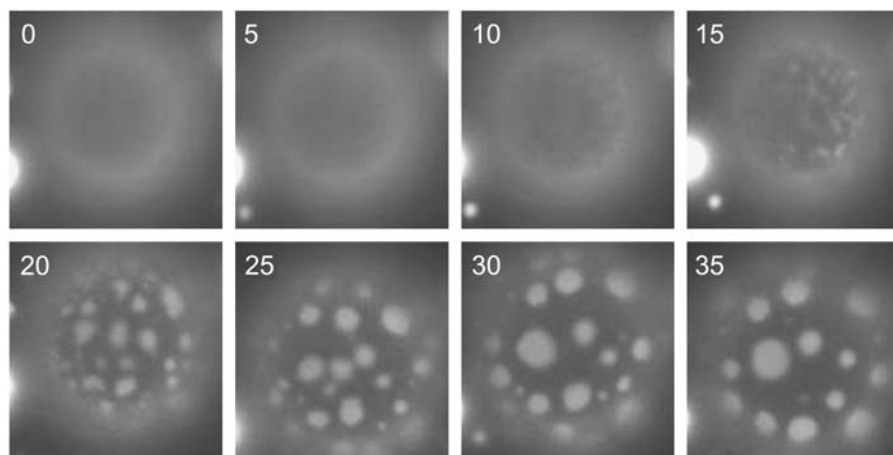10:20%, 20:20%, and 20:40%, we lowered temperature from

FIGURE 2 Photooxidation promotes large rafts for high cholesterol content bilayers. In the absence of antioxidants, large rafts formed within 15 s after illumination. GUVs prepared as in Fig. 1. Rho-DOPE was used as probe, so here nonraft circular domains are surrounded by a raft region. The times after starting illumination are shown (in units of seconds) in the upper left corners.

60°C to 25°C and scored the fraction of GUVs that presented large rafts. Visible domains were readily formed in all liposomes for the 20:10% SM/cholesterol mixture (Fig. 3 A). The raft region would bud and often pinch off for those liposomes that exhibited excess area, demonstrating that these rafts had high line tension (33). For SM/cholesterol at 20:20%, very few GUVs exhibited visible rafts (Fig. 3 B). But further lowering temperature, to ~15°C, did result in the appearance of large rafts (data not shown). As was the case for an SM/cholesterol ratio of 20:40%, microscopically visible rafts were not observed for a 10:20% mixture at 25°C (Fig. 3 C), but a few very small rafts did appear at 10°C. Clearly, increasing cholesterol concentration at a fixed amount of SM can eliminate large raft formation; this is consistent with phase diagrams characterizing small and large domains formed from DOPC/SM/cholesterol (34,35) and DOPC/DPPC/cholesterol mixtures (20). It has been common to use a 1:1:1 DOPC/SM/cholesterol mixture for raft studies in model bilayer membranes (14,36). (Although this has become a ''canonical'' lipid mixture, its SM content is higher and cholesterol content is lower than that of cell plasma membranes.) We found that for this mixture, large rafts readily formed in all the GUVs, even when the antioxidant NPG and the transition metal chelator DTPA

were included. Budding of rafts and other raft phenomena were similar to those of a 20:10% SM/cholesterol mixture, but the rafts were larger for the 1:1:1 mix. For SM/cholesterol percentages that did not require photooxidation for large rafts to form, intentional photooxidation induced the appearance of additional rafts. These new rafts merged among themselves as well as with preexisting rafts. Thus, photooxidation caused the total microscopically observed raft area to increase. (At no time did the entire bilayer become one large raft.) For monolayers composed of cholesterol and a saturated PC, the critical pressure for two microscopically visible, coexisting liquid phases decreased with lipid oxidation (37). In other words, here too, lipid oxidation promoted formation of large domains.

In the absence of NPG, rafts formed quickly for the 20:40% SM/cholesterol mixes, before there were appreciable decreases in fluorescence, independent of whether NBD-DPPE or Rho-DOPE was excited. (But bleaching of NBD-DPPE fluorescence was the much quicker of the two.) Thus, photobleaching of the probe was not the cause of the appearance of large rafts. If the incident light was blocked once rafts were observed, the preexisting rafts would merge among themselves, but additional rafts did not appear. If, instead, illumination was maintained, new rafts continued to form and merge and a greater percentage of the GUV membrane formed a raft. When the photoinduced rafts first formed, line tension was small as indicated by large fluctuations in raft boundaries that deviated from a circular shape. The undulations of the boundary decreased with time of illumination. The magnitude of undulations should depend on line tension and not on hydrostatic pressure within a vesicle. (This is advantageous because pressure is difficult to measure or to control for a GUV.) The decreasing undulations show that continued photooxidation leads to greater line tension.

When NPG was present, fluorescence of Rho-DOPE had to decrease ~20% from its initial value before large rafts formed. This need for significant photobleaching in the presence of NPG, but not in its absence, indicates that
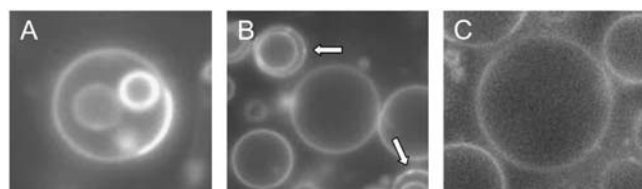

FIGURE 3 In the absence of photooxidation, the appearance of large rafts depended on the ratios of SM and cholesterol rather than on a simple increase in the amounts of the two components. (A) Large rafts formed for a 20:10% SM/cholesterol mixture. (B) Large rafts were scarce for a 20:20% SM/cholesterol mixture. Small, barely visible rafts are marked by arrows. (C) Large rafts were absent for a 10:20% mixture. NBD-DPPE was used as probe for this figure. All images are for GUVs at 25°C.

excitation of rhodamine (which should reside in the aqueous phase) initiates chain reactions that lead to products that cause the creation of large rafts; NPG terminates the reactions, preventing the production of these products until considerable photobleaching occurs. This has practical consequences. For example, lipid oxidation must occur in fluorescence recovery after photobleaching (FRAP) experiments, limiting the suitability of FRAP for raft study.

Small rafts that do not enlarge form without photooxidation

The question naturally arises: For lipid mixtures that do not exhibit microscopically observable rafts, does photooxidation create the rafts or does it promote the enlargement of preexisting small, nanoscopic rafts? A standard procedure for identifying whether a lipid mixture yields small rafts at a given temperature is to measure, in cuvette fluorimetry experiments, the FRET signal between a probe that concentrates in rafts (e.g., NBD-DPPE as donor) and one that remains in the surround (e.g., Rho-DOPE acceptor), or vice versa (18,19): at constant temperature, raft formation lowers the FRET acceptor signal as compared to probes uniformly distributed. Unlike fluorescence microscopy, cuvette-fluorescence spectroscopy is basically not susceptible to photooxidation. In cuvette experiments, vesicles continuously move through the beam of illumination, beam intensity is low, small amounts of probe are used, and solutions are purged of oxygen and sealed within cuvettes—so if rafts formed in these experiments, photooxidation could not be the cause.

We attempted to generalize the constant temperature FRET procedure to identify raft formation upon lowering temperature. We formed 200-nm-diameter unilamellar vesicles at ~60°C and lowered temperature to below T_m. For vesicles containing SM (eSM/DOPC, 1:4) and a high concentration of NBD-DPPE (3 mol %), but free of cholesterol, NBD fluorescence was constant as temperature was lowered to just below 40°C (T_m of 16:0 SM, ~41°C) (Fig. 4, inset). As temperature was lowered further, fluorescence continuously decreased with the same slope at all temperatures. The decrease in fluorescence is accounted for by separation of SM into a solid-ordered phase below 40°C: NBD-DPPE preferentially partitions into a SM solid-ordered phase (32). The greater self-quenching that results from the inclusion of NBD-DPPE into this phase accounts for the decrease in fluorescence with lowered temperature. Because probe fluorescence should be intrinsically independent of temperature, the total area occupied by SM in a solid-ordered phase appears to have continually increased with lowered temperature.

The fluorescence of NBD-DPPE (as a sole probe) continuously increased as temperature was lowered, even at a concentration as low as 0.1 mol % of probe, in a 20%/40% eSM/cholesterol lipid mixture (Fig. 4, open circles). The temperature dependence above 40°C was surprising because rafts should not continuously form and/or enlarge at tem-
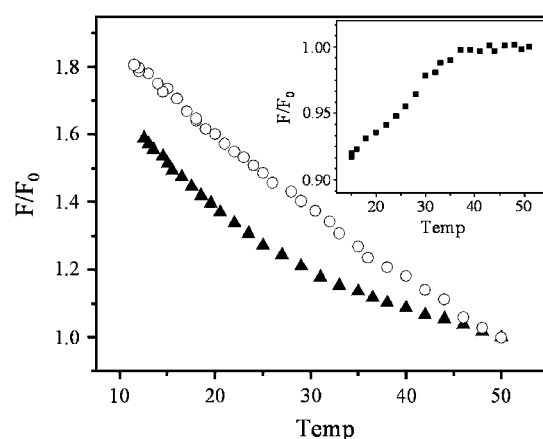

FIGURE 4 Using fluorimetry to measure the formation of small rafts upon lowering temperature. Liposomes of 200-nm diameter were prepared from a 20%/40%/40% eSM/cholesterol/DOPC mixture. For liposomes containing NBD-DPPE (0.1%) as a sole probe (open circles), fluorescence varies with the same slope for temperatures above and below 40°C. In contrast, partially quenching the NBD-DPPE fluorescence by Rho-DOPE (1%) caused NBD fluorescence to increase more steeply below 30°C–35°C than above this temperature range (solid triangles). The unquenched (open circles) and quenched (solid triangles) fluorescence was normalized to their values at 50°C, plotted as F/F_0. Records are shown for a typical experiment. Inset: NBD-DPPE fluorescence in liposomes composed of eSM/DOPC 20:80%, illustrated for a typical experiment.

peratures above T_m. The increase was observed for temperatures significantly >40°C and the slope of the increase was independent of temperature, with no changes from 50°C down to 10°C. The fluorescence of Rho-DOPE (in the absence of NBD-DPPE) exhibited a similar, but much less severe, variation with temperature, but here fluorescence decreased with lowered temperature (data not shown). The data thus indicate that the fluorescence of each of the probes can vary with extremely subtle changes in lipid packing in the presence of SM and cholesterol. Independent of the cause of fluorescence changes, a change in a FRET signal would not be an unambiguous signifier of raft formation as temperature is lowered. We therefore developed an alternate procedure to detect the onset of rafts upon temperature lowering.

We included each of the probes (0.1% NBD-DPPE and 1% Rho-DOPE) in vesicle preparations, but rather than utilizing FRET, we employed this relatively low amount of Rho-DOPE as a partial quencher of NBD fluorescence: if a raft forms, the inclusion of NBD-DPPE and exclusion of Rho-DOPE within the raft should relieve quenching of NBD and result in a fluorescence increase greater than would be caused by subtle packing changes. We found that the quenched signal increased more steeply for temperatures below ~30°C than above (Fig. 4, solid triangles). This change in slope at temperatures <30°C clearly distinguishes it from the uniform increase in fluorescence with lowered temperature where NBD-DPPE is the sole probe (open circles). Also, above 30°C, the quenched NBD-DPPE fluorescence was relatively independent of temperature. This is consistent with the

expectation that NBD-DPPE and Rho-DOPE remain in a single phase above the transition temperature for raft formation. The change in slope for temperatures below 30°C shows that the two probes became physically more separated from each other, relieving the quenching. In other words, as rafts formed, NBD-DPPE preferentially partitioned into them and Rho-DOPE remained in the surround. The continual increase in slope below 30°C is consistent with continual raft enlargement: as a raft enlarges, a smaller percentage of the NBD-DPPE resides at the raft boundary where it is quenched by Rho-DOPE in the surround. We thus conclude that small rafts do form for a 20%/40% SM/cholesterol mix in the absence of photooxidation. Lipid-oxidation may augment raft formation; it definitely promotes raft enlargement.

Breakdown products of SM-peroxide promote large raft formation

Our experiments and those of others (18–20) show that for some lipid compositions, small nanoscopic scale domains form but do not enlarge. The products induced by photooxidation should be responsible for raft enlargement for these compositions. Lipids photooxidize at double-bonded carbons to create lipid peroxides (38). Therefore SM, cholesterol, and DOPC can be peroxidized. Peroxides are unstable, breaking down into free radicals that can react with each other and with other lipids. We determined whether breakdown products of peroxides of SM and/or DOPC are responsible for raft enlargement. We generated peroxides from sonicated unilamellar vesicles composed of only SM or DOPC. As controls, we also prepared vesicles composed of DMPC and either SM or DOPC. We generated peroxides for each lipid mix by adding 10–20 μM chlorophyllin to a solution containing vesicles, and then we illuminated the preparation. The chlorphyllin served as a photosensitizer to generate peroxides. We partitioned the peroxides into water, measured their content, and catalyzed their breakdown into hydroxylated products by a Fe^{2+}-catalyzed Haber-Weiss reaction (see Materials and Methods). Each batch of peroxide breakdown products was separately included in a lipid mix (56% DOPC, 20% SM, 40% cholesterol, 1% Rho-DOPE, and 3% NBD-DPPE) and GUVs prepared. The addition of the SM-peroxide products (~5 mol %) consistently caused large rafts to form at 25°C (Fig. 5 A). The percentage of GUVs that exhibited rafts increased with lowered temperature (Fig. 5 B). The products of SM-peroxide were relatively insoluble in solvents (see Materials and Methods) and this may have caused them to distribute nonuniformly throughout the vesicle population. Such nonuniformity may have contributed to the appearance of large rafts in only a fraction of the GUVs. (Products were solubilized in the presence of either sulfuric acid or acetic acid. Those solubilized by sulfuric acid induced large rafts at somewhat higher temperatures than those solubilized by acetic acid. But a larger percentage of the GUVs containing
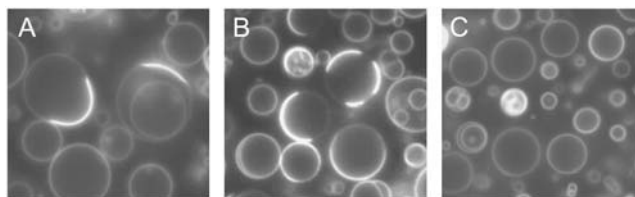

FIGURE 5 Breakdown products of SM-peroxide, but not those of DOPC-peroxide, induce raft enlargement. (A) GUVs that included 5 mol % of SM-peroxide breakdown products in a 15:40:36% eSM/cholesterol/DOPC (plus 1% NBD-DPPE and 3% Rho-DOPE) mixture yielded large rafts at 25°C. (B) A greater percentage of the GUVs exhibited rafts at 10°C (C). GUVs that included 10 mol % of DOPC-peroxide products in a 20:40:26% eSM/ cholesterol/DOPC (plus 1% NBD-DPPE and 3% Rho-DOPE) mixture did not yield visible rafts, even when temperature was lowered to 1°C. Note that the lipid mixtures were the same in all cases, except that in panels A and B the 5 mol % of SM-peroxide breakdown products replaced an equivalent amount of SM, whereas in (C) the 10 mol % DOPC-peroxide breakdown products substituted for this amount of DOPC. All three images display the fluorescence of NBD-DPPE.

the acetic acid-solubilized products exhibited large rafts at lower temperatures. It is likely that incorporation was less uniform for the sulfuric acid-solubilized products.) The large rafts that did appear were generated even though 2 mM NPG was present at all stages of the experiment, commencing with the initial step of drying the lipid-solvent mix to prepare GUVs. In control experiments, we showed that any Fe^{2+}/ Fe^{3+} that may have been present along with the products did not induce large rafts (see Materials and Methods). Also, the same results were obtained when we continually included 100 μM DTPA (starting from GUV formation) as a chelator to prevent the possibility of iron-catalyzed autoxidations (29). In contrast to SM, including up to 10 mol % of DOPC, breakdown products in the same lipid mixture did not result in the formation of large rafts, down to temperatures as low as 1°C (Fig. 5 C). This contrasts with the finding that large rafts did form at this temperature when the DOPC breakdown products were not included. In conclusion, we have shown that breakdown products of SM-peroxide cause raft enlargement. But not all peroxide breakdown products induce raft enlargement. If small rafts did form in the absence of peroxidation for our 20:40% SM/cholesterol mixture, products of peroxide breakdown did not serve as nucleation centers for phase separation, but rather became raft components that promoted raft enlargement. Preferential partitioning of an oxidation product into a phase caused by favorable interactions could explain why an oxidation product promotes domain enlargement. We emphasize that the raft enlargement was induced without any photooxidation whatsoever— breakdown products isolated from separate photosensitized preparations caused the enlargement.

Peroxides can form during GUV production

In addition to photooxidation upon excitation of photosensitizers such as fluorescent lipids, lipid peroxides can be

created as a consequence of electrochemical reactions. In preparing GUVs by electroswelling, voltages are applied to electrodes that serve as capacitor plates. Electron transfer can occur at these electrodes, leading to electrolysis and other electrochemical reactions that produce peroxides (39).

ITO-coated glass has become the standard electrode for generating GUVs used in raft studies (14,22,33). We initially used this ITO-glass for electroswelling, but after discovering the importance of peroxide production in raft enlargement, we tested whether peroxides were created when using this electrode. We prepared GUVs containing eSM/cholesterol/DOPC (20:20:60%), measured peroxide levels, and normalized to the amount of lipid. (To prevent any possibility of photoinduced peroxidation, fluorescent lipids were not included.) For ITO-glass electrodes, ~0.6 mol % of lipid-peroxide was produced for solutions that had been purged of O_2 (Fig. 6, bar graphs, first column). (The solutions were not, however, isolated from air during the electroswelling at 60°C.) Because of chain reactions (see Discussion), this level of peroxide content could lead to products that induce large rafts for some lipid compositions that would not otherwise lead to rafts. We therefore switched to titanium (Ti) electrodes because the oxide (TiO_2) that naturally forms and that tightly adheres to the metallic surface blocks current at anodes (40). Oxidation (electron transfer from solution into the electrode) occurs at anodes, and so the use of titanium electrodes should not result in peroxides. We explicitly checked this by measuring peroxide levels for the GUVs prepared using titanium electrodes, and found that peroxide levels were below the measurable limit of our assay (Fig. 6, bar graphs, second column).

We tested whether the choice of electrodes in preparing GUVs was consequential to raft enlargement: we used ITO-glass and titanium as electrodes to prepare separate batches of GUVs by standard electroswelling procedures (22) for a 20:40:40% SM/cholesterol/DOPC mixture. We ensured that all conditions were equivalent except for the choice of electrodes by simultaneously preparing the GUVs with the same apparatus, using separate chambers for each electrode system. Large rafts formed at 25°C for ~20% of the GUVs prepared by ITO-glass (Fig. 6 A); no rafts were observed for those prepared by titanium. At ~5°C, a greater percentage of the ITO-glass GUVs exhibited large rafts (Fig. 6 B); titanium GUVs were still completely free of rafts (Fig. 6 C). The generation of peroxides for GUVs made by electroswelling using ITO-glass electrodes is undoubtedly the cause of the large rafts for the 20:40% SM/cholesterol lipid mixture. (It is not surprising that a fraction of the GUVs prepared with ITO-glass did not exhibit rafts because only GUVs that came into proximity with the electrodes could have their lipids peroxidized.) Because we now know that the use of ITO-glass electrodes leads to peroxides and that peroxides break down to yield free radicals that lead to a large amount of oxidation products, these electrodes should not be used to generate GUVs containing unsaturated lipids, regardless of
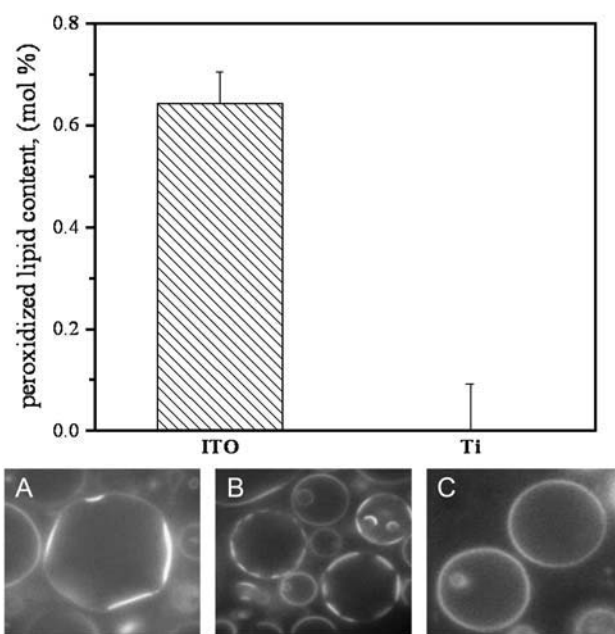

FIGURE 6 Forming GUVs with ITO-glass electrodes, but not with titanium electrodes, generates peroxides. Bar graph: ITO-glass and titanium electrodes were used to prepare GUVs composed of 20:20:60% eSM/cholesterol/DOPC, and peroxide content was measured by a FOX assay and normalized to the amount of lipid. (This amount was calculated from the measured phospholipid content.) The ordinate thus displays the percentage of peroxide relative to the total lipid content in mol %. Error bar is mean ± SE, $n = 4$. The use of ITO-glass led to peroxides (column 1), but titanium electrodes (column 2) did not generate peroxides. GUVs were prepared in 200 mM sucrose using a 3 V p-p, 10-Hz sine wave across the electrodes. Images: When ITO-glass electrodes were used to prepare GUVs composed of 20:40:40% eSM/cholesterol/DOPC, some large rafts formed at 25°C (A); more formed at 4°C (B). Only a fraction of the GUVs could exhibit rafts because only those vesicles that came within proximity of the electrodes could have their lipids electrochemically peroxidized. Preparing GUVs under precisely the same conditions, but using titanium electrodes, did not lead to rafts, shown here at 10°C (C; see also Fig. 1). NBD-DPPE was used as probe for all images.

the intended application of the GUVs. Since titanium electrodes do not generate peroxides, they are suitable for GUV preparation by electroswelling.

Raft behavior is different in GUVs and directly adhered bilayers

Planar bilayers supported by a solid substrate provide a thin optical section convenient for fluorescence microscopy, and this system is often used for raft study (14,32,41). We therefore tested the consequences of photooxidation on raft enlargement in this system, using a 20:20% eSM/cholesterol mix containing 1% Rho-DOPE and 3% NBD-DPPE as probes. For bilayers formed directly on a mica substrate (mica was chosen because it is molecularly flat (42)), the fluorescence of both probes was microscopically uniform at high temperature (55°C). In the presence of antioxidants

(NPG or ascorbate), irregularly shaped small domains (~1–2 μm) depleted of Rho-DOPE and enriched in NBD-DPPE formed when temperature was lowered to 25°C. This formation of visually observable domains is in contrast with the lack of observable rafts in GUVs for the same lipid mix (Fig. 7 *A*). When antioxidants were omitted from the supported bilayer system, illumination for a few minutes affected the appearance of the domains: the region of the bilayer exposed to the incident light exhibited larger and less densely spaced rafts than the nonilluminated regions. Also, at the circular boundary of the illuminated area, a ring of thickness of few microns appeared that did not contain any rafts (Fig. 7 *B*). In the presence of antioxidants, rafts within and outside the illuminated area were the same, and this ring did not form.

FRAP experiments using fringe pattern and small diameter beams (~1 μm) have previously demonstrated that the individual lipids within the monolayer apposing the substrate are not immobilized by their interactions with the substrate (32,43). We found that photobleaching large areas (~20 μm) of the bilayer at high temperature (i.e., fluorescence was uniform) led to full fluorescence recovery within a few minutes. This indicates that large regions of the adhered bilayer were continuous, rather than comprising separate patches of membrane, and confirms that individual lipids in both monolayers were mobile. But we also found that despite

the free diffusion of individual lipids, rafts were immobile, as has been described by others (32,44). The immobility of rafts obviously prevented their merger and thus rafts could not substantially enlarge over time. The contrast between formation and enlargement of rafts in GUVs and supported bilayers shows that interactions of a bilayer with a substrate can dominate raft properties. This is similar to the demonstration that for a dipalmitoylphosphatidylcholine/dilauryl-phophatidylcholine/cholesterol mixture, phase separation into liquid crystalline and gel phases occurs more readily for a planar bilayer directly adhered to a mica support than for a free GUV (23).

Rafts in cushioned bilayers are similar to those in GUVs

We reduced the bilayer mica interactions by using one of two polymers, one MW ~1,800 and the other MW ~65,000, to make a "cushion" between the bilayer and the mica substrate. The thickness of the cushion created by the small polymer is 11–15 nm (26); the thickness of the cushion created by the larger polymer has not been measured, but it is likely to be substantially greater. For the smaller polymer, rafts formed in a manner that was generally similar to that in bilayers directly supported by the substrate. However, these rafts were larger and more "rounded" than the irregularly shaped rafts observed without polymer. In the absence of antioxidant, illumination caused raft enlargement. After a few minutes, rafts within an illuminated region were somewhat larger than those in the nonilluminated surrounding bilayer. Visible rafts were immobile, and so their enlargement must have occurred through accretion of material from the surround. Calculations show that raft enlargement through accumulation of monomeric lipids into micron scale domains (e.g., enlargement via Ostwald ripening) is extremely slow (45). We therefore assume that submicroscopic rafts were present, and they were sufficiently mobile to reach and merge with the visible rafts.

When the larger polymer was used to create a cushion to separate bilayer from substrate, microscopically visible rafts did not form at 25°C if antioxidants were present (Fig. 7 *C*). (Further lowering temperature to 10–15°C led to a few, barely resolvable rafts.) Photooxidation, induced by increasing illumination intensity or omitting antioxidants, readily caused large rafts to form (Fig. 7 *D*). The rafts were not perfectly circular, but they were much less irregularly shaped than those within bilayers directly adhered to a substrate. The rafts were mobile, but less mobile than for GUVs. They rapidly merged upon contact with each other. Raft enlargement also occurred without observable mergers. Here again, accretion of material from the surround must be responsible for this enlargement. In short, the properties of rafts within planar bilayers separated from substrate by a thick cushion were basically the same as for rafts in GUVs. Our results show that adhesive interactions between a bilayer and
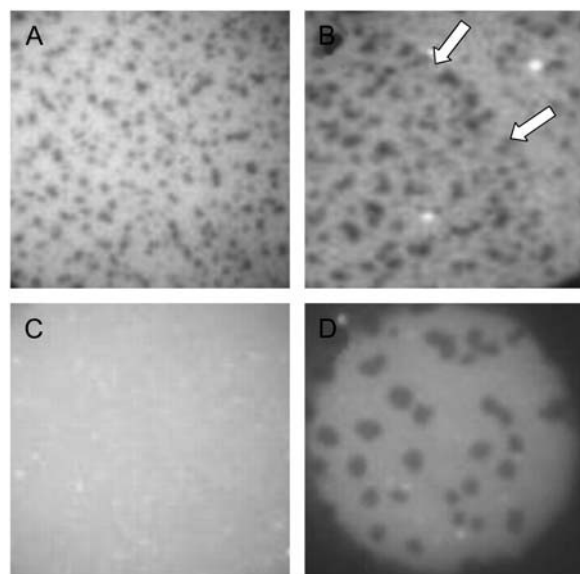

FIGURE 7 Adhering a bilayer directly onto a substrate promotes large rafts. (*A*) For a 20:20:40:20% eSM/cholesterol/DOPC/DOPE bilayer adhered to a mica substrate, large rafts form at 25°C in the presence of antioxidants. (This contrasts to GUVs of the same composition, for which rafts did not form.) (*B*) Photooxidation produced by illumination in the absence of antioxidants led to larger rafts. The arrows mark the boundary of the illuminated area. (*C*) Providing a cushion (here, made with 65 kD PEI) between the bilayer and substrate reduces large raft formation. In the presence of antioxidants, large rafts do not appear at 25°C for a cushioned bilayer. (*D*) Rafts appear in the cushioned bilayer when photooxidation is not prevented. Rho-DOPE was used as probe.

substrate greatly alter some raft properties and that polymer cushions can be used to minimize, but not completely eliminate, the consequences of bilayer interactions with the substrate. These experiments also emphasize that photooxidation induces the formation of large rafts in free, noninteracting lipid bilayers, independent of the precise model system employed.

DISCUSSION

In this study, we have shown that it is imperative to employ photoprotectors in lipid raft studies to accurately determine raft growth and raft properties, such as line tension. We demonstrated that for some lipid compositions, large rafts appear only if photooxidation occurs. For lipid compositions that do not require photooxidation for large rafts to form, photooxidation still has the effect of increasing raft line tension. We further demonstrated that the formation of photoinduced large rafts is caused by the presence of breakdown products of peroxides, predominantly SM-peroxides. In addition to lipid peroxide production by photooxidation, lipid peroxides can also be generated by electrochemical reactions during the electroswelling used to create GUVs—a problem that can be avoided by employing titanium electrodes.

Photochemical production of peroxides

Several groups have determined the phase diagrams for raft formation in lipid bilayer membranes, at a given temperature, as a function of lipid composition (16,21,32,46). A phase diagram identifies the compositions that yield small nanodomains, large microscopically observable domains, and compositions in which small and large domains coexist. It has been argued that photooxidation of lipid mixtures is not of practical consequence in phase separation studies in lipid bilayers, other than changing the transition temperature and that photooxidation does not affect the formation of large domains within bilayers when cholesterol is the only double-bonded lipid (47). This study stands in stark contrast to these assertions and shows that if photooxidation is allowed to proceed, data and conclusions can be seriously corrupted. But our study is in accord with many investigations that show that lipid peroxidation can greatly affect a wide range of membrane properties, including increasing membrane permeability and fluidity (48). Recently, it has also been shown, by x-ray diffraction, that lipid peroxidation alters cholesterol organization and distribution within bilayer membranes (49).

Excitation of lipid fluorophores unquestionably produces peroxides. The mechanisms are well understood (38). Fluorescent dyes have singlet ground states; molecular oxygen's (O_2) ground state is a triplet. After photon absorption excites the dye into its lowest singlet state, there is a low, but finite, probability that the dye decays to an excited triplet state via intersystem crossing with spin inversion. The triplet state is relatively long lived and can transfer its energy to ground state triplet O_2, elevating molecular oxygen to its excited singlet state (Fig. 8). The excited singlet O_2 reacts with double-bonded carbons (always singlet states) to generate lipid peroxides without prior creation of free radicals. Because O_2 can dissolve in a hydrocarbon medium, the excited state O_2 could readily react with any lipid carbon double bonds.

The general consequences of peroxide production on nonperoxidized lipids are also quite well known (Fig. 8). In fluorescence microscopy experiments, peroxides will spontaneously decay to free radicals because the oxygen-oxygen bond of a peroxide is quickly broken in the presence of trace amounts of catalytic transition metals (e.g., Fe^{2+}, Cu^{2+})
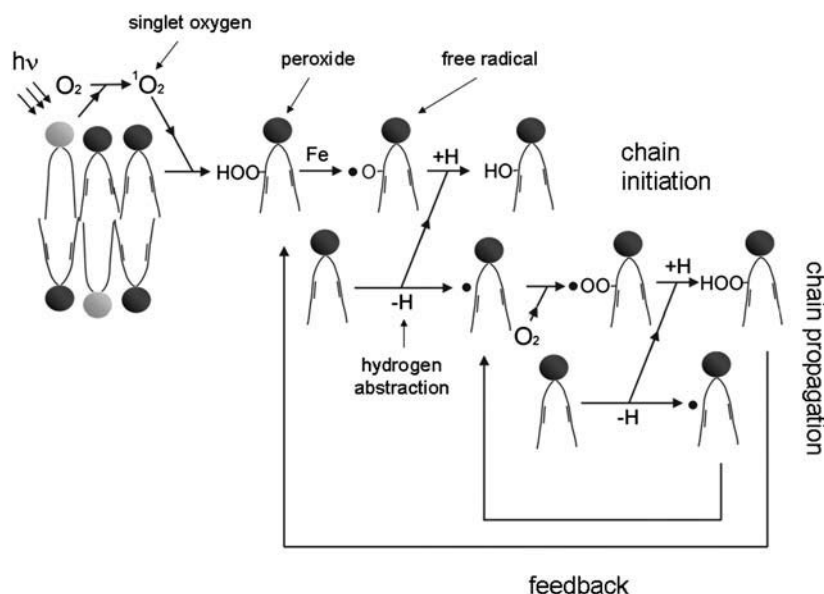

FIGURE 8 Photoexcitation of a fluorescent probe results in a cascade of reactions. One such cascade is illustrated. A photoexcited fluorescent probe raises molecular oxygen to its singlet excited state. The excited oxygen reacts with a double bond on an acyl chain to create a peroxide. The peroxide is unstable in the presence of any trace ferrous (or other transition metals) and decays to a lipid-free radical which removes (i.e., abstracts) a hydrogen from an unoxidized, unsaturated lipid. This creates a hydroxylated lipid (i.e., a peroxide product) and a new free radical. Molecular oxygen combines with the new radical, abstracting a hydrogen from another unsaturated lipid, and again producing a free radical and a lipid peroxide. This free radical and lipid peroxide initiates an additional round of reactions. The two feedback loops result in substantial lipid oxidation. These reactions occur without any destruction of the excited fluorescent lipid probe that decays back to its ground state, from which it can again be photoexcited.

(29). The decay initiates a chain reaction. The free radical with its unpaired electron readily reacts with electrons of carbon-carbon double bonds and other groups, producing secondary free radicals that in turn react with many lipids in a diffusion-limited chain reaction (Fig. 8). The chain reaction ceases only after free radicals combine with each other. Antioxidants eliminate the lipid-free radicals by donating a hydrogen atom to the radical. That is, the lipid-free radical abstracts a hydrogen from the antioxidant rather than from an unsaturated lipid (chain initiation, Fig. 8); this prevents propagation of the chain reaction. Ideally, only a single hydroxylated lipid is generated in the presence of antioxidants. In the absence of antioxidants, chain reactions cause many lipids to be modified. In peroxide-initiated chain reactions, the free radicals replenish themselves via feedback loops. In the cascade we illustrate, there are two such loops (Fig. 8). As a result of these amplifications, production of small amounts of lipid peroxides modifies a large percentage of the membrane lipids unless explicit means of prevention are taken.

If lipid peroxides are produced by any means—photooxidation, electroswelling, or during lipid storage—all unsaturated lipids can be converted into a myriad of oxidation products. Cholesterol readily undergoes autoxidization and peroxidation to give rise to oxysterols of various structures including 5-hydroxy cholesterol (51). Thus, even if cholesterol is the only unsaturated lipid in a bilayer membrane, its oxidation could, in principle, be the cause of formation of large domains in fluorescence microscopy experiments. Also, lowering of cholesterol content by oxidation could promote phase separation, as previously suggested (50).

We included a small number of products—those that can be produced by a Haber-Weiss reaction—in GUVs to demonstrate that oxidation products can cause large rafts. In fluorescence microscopy experiments, many more products are almost certainly generated if photooxidation occurs. For example, in addition to products of Haber-Weiss reactions, lipid cleavage can occur, epoxides are probably produced, and a Russell reaction should proceed (38). This proliferation of photooxidized compounds should lead to more pronounced effects on raft size than does incorporation of a small amount of a few products, and this in fact is the experimental finding. Importantly, generating many products leads to a new system—quite different in composition from the original—that cannot, as a practical matter, be characterized.

A simple estimation illustrates how much peroxide can be produced within seconds of illumination: Conservatively, $\sim 1\%$ of the excited fluorescent probes are in a triplet state (fluorescein has $\sim 3\%$ based on rates of fluorescence emission and intersystem crossing (52)). For 10^4 excitations/probe/s (a reasonable estimate), ~ 100 triplet states/probe/s are generated. Even if only 1% of these triplet states nonradiatively transfer energy to ground state O_2, one excited singlet O_2/probe/s is produced. For a concentration of 1% probe in the membrane and assuming that half of the excited singlet O_2 diffuses away from the membrane and the

other half diffuses toward it, reaction of the membrane-dissolved excited O_2 with lipids will cause 0.5% of the unsaturated lipids to be peroxidized every second. Unless a saturating concentration of antioxidants is present to immediately terminate all peroxide-initiated chain reactions, an appreciable amount of products will be quickly produced. This accounts for the experimental observation that, in the absence of antioxidants, photoillumination can quickly cause large rafts to appear. We emphasize that a fluorophore need not be chemically modified for large rafts to form by photoinduced oxidation. The mere transfer of energy from an excited fluorophore to ground state O_2 can lead to peroxides.

In summary, based on well-established chemical principles, photoexcitation will lead to lipid-peroxide production. Chain reactions must result from spontaneous decay of peroxides and these reactions will tremendously amplify the number of affected lipids. Our experiments clearly demonstrate that unless the chain reactions are prevented, the measured evolution and properties of rafts can be caused by experimentally uncontrolled chemical processes, rather than the intended phase separation of unoxidized lipids.

Electrochemical production of peroxides

Platinum electrodes were originally employed to prepare GUVs by electroswelling (53,54). These GUVs were used for studies unrelated to rafts. For raft studies, two ITO-coated glass slides are frequently used to create a parallel plate capacitor for producing GUVs. These glass slides are convenient because after electroswelling, the capacitor is mounted on a microscope and the GUVs viewed without the need for any disassembly (22). After finding that electrochemical reactions at ITO-glass electrodes yields lipid peroxides, we switched to titanium plates as capacitor electrodes, even though this necessitates removing the GUVs from between the capacitor plates and introducing them into a new chamber for microscopic visualizations. Titanium is sometimes referred to as a ''valve metal'' because its oxide layer at the surface minimizes ionic current at anodes (40). We showed that for our application, lipid peroxidation was effectively eliminated. (Platinum is not a valve metal, and we thus assume that it would lead to generation of peroxides.) Many specialized valve metal oxides have been developed as topcoats over electrodes for industrial applications (40), and so there should be a large range of suitable electrodes and topcoats. Titanium has the advantage that TiO_2, as a topcoat, forms spontaneously. Because the yields of GUVs were roughly the same for titanium as for ITO-glass electrodes, we evaluate titanium electrodes as reasonably optimal. Independent of choice of electrodes, it is imperative that they do not lead to production of peroxides during electroswelling.

Possible biological implications

To carry the implications of our findings beyond raft studies in model bilayer membranes, we note that:

First, fluorescent lipid analogs such as DiI or DiO are frequently used to monitor for rafts in cell plasma membranes (55,56). Obviously, photoinduced peroxidation could, in principle, alter the raft properties by means identical to or analogous to those elaborated in this study. However, tocopherol, native to cell membranes, probably serves as an antioxidant to prevent peroxide-induced chain reactions in biological systems.

Second, peroxide-initiated chain reactions result in the addition of molecular oxygen to lipids. For sphingolipids, the oxygen is added at the 4,5 double carbon bond of the sphingosine base. X-ray diffraction shows that the first three carbons of the sphingosine backbone are arranged in the same positions as the three glycerol carbons of phospholipids (57). It might be significant that an appreciable fraction (up to ~10% for some cell types) of sphingolipids in a plasma membrane is hydroxylated at the second carbon of the variable acyl chain (58,59). Because this carbon and the 4,5 double bond are similarly located with respect to the membrane-solution interface, the two hydroxylated forms of sphingolipids may affect raft properties in similar ways. If they do, the naturally occurring hydroxylated sphingolipids could provide a means for cells to quickly modulate raft size.

Third, there are many differences between cell and lipid bilayer membranes, and thus one can question whether a bilayer membrane provides a useful model system for raft study. It had been thought that large rafts form in bilayers containing levels of cholesterol comparable to those in cells (14,22,33). The absence of large rafts in cells therefore challenged the utility of the model system for raft study. Our demonstration that unoxidized lipids form small rafts, but not large ones, at a physiological percentage of cholesterol (~40 mol %) and sphingolipids (~20 mol %) indicates that essentially the same physics underlie bilayer and biological raft formation. If this is true, lipid bilayers provide a well-defined model system to reliably identify the physical forces that control the formation and size of rafts in biological membranes.

REFERENCES

1. Edidin, M. 2003. The state of lipid rafts: from model membranes to cells. *Annu. Rev. Biophys. Biomol. Struct.* 32:257–283.

2. He, H. T., A. Lellouch, and D. Marguet. 2005. Lipid rafts and the initiation of T cell receptor signaling. *Semin. Immunol.* 17:23–33.

3. Parton, R. G., and A. A. Richards. 2003. Lipid rafts and caveolae as portals for endocytosis: new insights and common mechanisms. *Traffic.* 4:724–738.

4. Young, R. M., X. Zheng, D. Holowka, and B. Baird. 2005. Reconstitution of regulated phosphorylation of FcepsilonRI by a lipid raft-excluded protein-tyrosine phosphatase. *J. Biol. Chem.* 280:1230–1235.

5. Kusumi, A., and K. Suzuki. 2005. Toward understanding the dynamics of membrane-raft-based molecular interactions. *Biochim. Biophys. Acta.* 1746:234–251.

6. Plowman, S. J., C. Muncke, R. G. Parton, and J. F. Hancock. 2005. H-ras, K-ras, and inner plasma membrane raft proteins operate in nanoclusters with differential dependence on the actin cytoskeleton. *Proc. Natl. Acad. Sci. USA.* 102:15500–15505.

7. Pralle, A., P. Keller, E. L. Florin, K. Simons, and J. K. Horber. 2000. Sphingolipid-cholesterol rafts diffuse as small entities in the plasma membrane of mammalian cells. *J. Cell Biol.* 148:997–1008.

8. Sharma, P., R. Varma, R. C. Sarasij, Ira, K. Gousset, G. Krishnamoorthy, M. Rao, and S. Mayor. 2004. Nanoscale organization of multiple GPI-anchored proteins in living cell membranes. *Cell.* 116:577–589.

9. Dietrich, C., B. Yang, T. Fujiwara, A. Kusumi, and K. Jacobson. 2002. Relationship of lipid rafts to transient confinement zones detected by single particle tracking. *Biophys. J.* 82:274–284.

10. Hess, S. T., M. Kumar, A. Verma, J. Farrington, A. Kenworthy, and J. Zimmerberg. 2005. Quantitative electron microscopy and fluorescence spectroscopy of the membrane distribution of influenza hemagglutinin. *J. Cell Biol.* 169:965–976.

11. Gidwani, A., D. Holowka, and B. Baird. 2001. Fluorescence anisotropy measurements of lipid order in plasma membranes and lipid rafts from RBL-2H3 mast cells. *Biochemistry.* 40:12422–12429.

12. London, E. 2005. How principles of domain formation in model membranes may explain ambiguities concerning lipid raft formation in cells. *Biochim. Biophys. Acta.* 1746:203–220.

13. Silvius, J. R. 2005. Partitioning of membrane molecules between raft and non-raft domains: insights from model-membrane studies. *Biochim. Biophys. Acta.* 1746:193–202.

14. Dietrich, C., L. A. Bagatolli, Z. N. Volovyk, N. L. Thompson, M. Levi, K. Jacobson, and E. Gratton. 2001. Lipid rafts reconstituted in model membranes. *Biophys. J.* 80:1417–1428.

15. Samsonov, A. V., I. Mihalyov, and F. S. Cohen. 2001. Characterization of cholesterol-sphingomyelin domains and their dynamics in bilayer membranes. *Biophys. J.* 81:1486–1500.

16. Veatch, S. L., and S. L. Keller. 2005. Miscibility phase diagrams of giant vesicles containing sphingomyelin. *Phys. Rev. Lett.* 94:148101.

17. de Almeida, R. F., L. M. Loura, A. Fedorov, and M. Prieto. 2005. Lipid rafts have different sizes depending on membrane composition: a time-resolved fluorescence resonance energy transfer study. *J. Mol. Biol.* 346:1109–1120.

18. Heberle, F. A., J. T. Buboltz, D. Stringer, and G. W. Feigenson. 2005. Fluorescence methods to detect phase boundaries in lipid bilayer mixtures. *Biochim. Biophys. Acta.* 1746:186–192.

19. Silvius, J. R. 2003. Fluorescence energy transfer reveals microdomain formation at physiological temperatures in lipid mixtures modeling the outer leaflet of the plasma membrane. *Biophys. J.* 85:1034–1045.

20. Veatch, S. L., I. V. Polozov, K. Gawrisch, and S. L. Keller. 2004. Liquid domains in vesicles investigated by NMR and fluorescence microscopy. *Biophys. J.* 86:2910–2922.

21. Feigenson, G. W., and J. T. Buboltz. 2001. Ternary phase diagram of dipalmitoyl-PC/dilauroyl-PC/cholesterol: nanoscopic domain formation driven by cholesterol. *Biophys. J.* 80:2775–2788.

22. Veatch, S. L., and S. L. Keller. 2003. Separation of liquid phases in giant vesicles of ternary mixtures of phospholipids and cholesterol. *Biophys. J.* 85:3074–3083.

23. Tokumasu, F., A. J. Jin, G. W. Feigenson, and J. A. Dvorak. 2003. Nanoscopic lipid domain dynamics revealed by atomic force microscopy. *Biophys. J.* 84:2609–2618.

24. MacDonald, R. C., R. I. MacDonald, B. P. Menco, K. Takeshita, N. K. Subbarao, and L. R. Hu. 1991. Small-volume extrusion apparatus for preparation of large, unilamellar vesicles. *Biochim. Biophys. Acta.* 1061:297–303.

25. Johnson, J. M., T. Ha, S. Chu, and S. G. Boxer. 2002. Early steps of supported bilayer formation probed by single vesicle fluorescence assays. *Biophys. J.* 83:3371–3379.

26. Wong, J. Y., J. Majewski, M. Seitz, C. K. Park, J. N. Israelachvili, and G. S. Smith. 1999. Polymer-cushioned bilayers. I. A structural study of various preparation methods using neutron reflectometry. *Biophys. J.* 77:1445–1457.

27. Wong, J. Y., C. K. Park, M. Seitz, and J. N. Israelachvili. 1999. Polymer-cushioned bilayers. II. An investigation of interaction forces and fusion using the surface forces apparatus. *Biophys. J.* 77:1458–1468.

28. Kamat, J. P., K. K. Boloor, and T. P. Devasagayam. 2000. Chlorophyllin as an effective antioxidant against membrane damage in vitro and ex vivo. *Biochim. Biophys. Acta.* 1487:113–127.

29. Buettner, G. R., and B. A. Jurkiewicz. 1996. Catalytic metals, ascorbate and free radicals: combinations to avoid. *Radiat. Res.* 145:532–541.

30. Stewart, J. C. 1980. Colorimetric determination of phospholipids with ammonium ferrothiocyanate. *Anal. Biochem.* 104:10–14.

31. Wolff, S. P. 1994. Ferrous ion oxidation in presence of ferric ion indicator Xylenol orange for measurement of hydroperoxides. *Methods Enzymol.* 233:182–189.

32. Crane, J. M., and L. K. Tamm. 2004. Role of cholesterol in the formation and nature of lipid rafts in planar and spherical model membranes. *Biophys. J.* 86:2965–2979.

33. Baumgart, T., S. T. Hess, and W. W. Webb. 2003. Imaging coexisting fluid domains in biomembrane models coupling curvature and line tension. *Nature.* 425:821–824.

34. Hammond, A. T., F. A. Heberle, T. Baumgart, D. Holowka, B. Baird, and G. W. Feigenson. 2005. Crosslinking a lipid raft component triggers liquid ordered-liquid disordered phase separation in model plasma membranes. *Proc. Natl. Acad. Sci. USA.* 102:6320–6325.

35. Kahya, N., D. Scherfeld, K. Bacia, B. Poolman, and P. Schwille. 2003. Probing lipid mobility of raft-exhibiting model membranes by fluorescence correlation spectroscopy. *J. Biol. Chem.* 278:28109–28115.

36. Veatch, S. L., and S. L. Keller. 2003. A closer look at the canonical 'Raft Mixture' in model membrane studies. *Biophys. J.* 84:725–726.

37. Benvegnu, D. J., and H. M. McConnell. 1993. Surface dipole densities in lipid monolayers. *J. Phys. Chem.* 97:6686–6691.

38. Girotti, A. W. 1990. Photodynamic lipid peroxidation in biological systems. *Photochem. Photobiol.* 51:497–509.

39. Harada, K. 2002. Behavior of hydrogen peroxide in electrolyzed anode water. *Biosci. Biotechnol. Biochem.* 66:1783–1791.

40. Eltech Systems Corporation. 2005. Mixed metal oxide anodes. www.lidaproducts.com.[Online].

41. Shaw, J. E., R. F. Epand, R. M. Epand, Z. Li, R. Bittman, and C. M. Yip. 2006. Correlated fluorescence-atomic force microscopy of membrane domains: structure of fluorescence probes determines lipid localization. *Biophys. J.* 90:2170–2178.

42. Israelachvili, J. N., and D. Tabor. 1972. The measurement of van der Waals dispersion forces in the range of 1.5 to 130 nm. *Proc. R. Soc. Lond. A.* 331:19–38.

43. Huang, Z., K. H. Pearce, and N. L. Thompson. 1994. Translational diffusion of bovine prothrombin fragment 1 weakly bound to supported planar membranes: measurement by total internal reflection with fluorescence pattern photobleaching recovery. *Biophys. J.* 67:1754–1766.

44. Stottrup, B. L., S. L. Veatch, and S. L. Keller. 2004. Nonequilibrium behavior in supported lipid membranes containing cholesterol. *Biophys. J.* 86:2942–2950.

45. Frolov, V. A., Y. A. Chizmadzhev, F. S. Cohen, and J. Zimmerberg. 2006. Entropic traps in the kinetics of phase separation in multicomponent membrane stabilize nanodomains. *Biophys. J.* 91:189–205.

46. de Almeida, R. F., A. Fedorov, and M. Prieto. 2003. Sphingomyelin/phosphatidylcholine/cholesterol phase diagram: boundaries and composition of lipid rafts. *Biophys. J.* 85:2406–2416.

47. Veatch, S. L., and S. L. Keller. 2005. Seeing spots: complex phase behavior in simple membranes. *Biochim. Biophys. Acta.* 1746:172–185.

48. Kunimoto, M., K. Inoue, and S. Nojima. 1981. Effect of ferrous ion and ascorbate-induced lipid peroxidation on liposomal membranes. *Biochim. Biophys. Acta.* 646:169–178.

49. Jacob, R. F., and R. P. Mason. 2005. Lipid peroxidation induces cholesterol domain formation in model membranes. *J. Biol. Chem.* 280:39380–39387.

50. Roax, A. D. Cuvelier, P. Nassoy, J. Prost, P. Basseredu, and B. Goud. 2005. Role of curvature and phase transition in lipid sorting and fission of membrane tubules. *EMBO J.* 24:1537–1545.

51. Korytowski, W., M. Wrona, and A. W. Girotti. 1999. Radiolabeled cholesterol as a reporter for assessing one-electron turnover of lipid hydroperoxides. *Anal. Biochem.* 270:123–132.

52. Song, L., C. A. Varma, J. W. Verhoeven, and H. J. Tanke. 1996. Influence of the triplet excited state on the photobleaching kinetics of fluorescein in microscopy. *Biophys. J.* 70:2959–2968.

53. Angelova, M., and D. Dimitrov. 1986. Liposome electroformation. *Faraday Discuss. Chem. Soc.* 81:303–311.

54. Dimitrov, D., and M. Angelova. 1987. Lipid swelling and liposome formation on solid surfaces in external electric fields. *Prog. Colloid Polym. Sci.* 73:48–56.

55. Bacia, K., D. Scherfeld, N. Kahya, and P. Schwille. 2004. Fluorescence correlation spectroscopy relates rafts in model and native membranes. *Biophys. J.* 87:1034–1043.

56. Hao, M., S. Mukherjee, and F. R. Maxfield. 2001. Cholesterol depletion induces large scale domain segregation in living cell membranes. *Proc. Natl. Acad. Sci. USA.* 98:13072–13077.

57. Pascher, I. 1976. Molecular arrangements in sphingolipids. Conformation and hydrogen bonding of ceramide and their implication on membrane stability and permeability. *Biochim. Biophys. Acta.* 455:433–451.

58. De Haas, C. G., and M. Lopes-Cardozo. 1995. Hydroxy- and non-hydroxy-galactolipids in developing rat CNS. *Int. J. Dev. Neurosci.* 13:447–454.

59. O'Brien, J. S., D. L. Fillerup, and J. F. Mead. 1964. Quantification and fatty acid and fatty aldehyde composition of ethanolamine, choline, and serine glycerophosphatides in human cerebral grey and white matter. *J. Lipid Res.* 5:329–338.